Sensorless Synchronous Motor Drive for Use on Commercial Transport Airplanes

Farhad Nozari, *Senior Member, IEEE*, Paul A. Mezs, *Member, IEEE*, Alexander L. Julian, Chiping Sun, and Thomas A. Lipo, *Fellow, IEEE*

Abstract—**This paper describes a sensorless synchronous machine drive to be used for starting an auxiliary power unit (APU) on commercial transport airplanes. The proposed method utilizes the synchronous generator mounted on the APU, and presently only used as a source of electrical power, as a synchronous motor for starting the APU. The developed sensorless synchronous motor drive starting function involves measurement of machine terminal voltage and current, from which the desired current command is then calculated and implemented by the drive converter. Power into the machine is determined by a power control loop, while the system voltage is limited to a desired value by a field weakening loop in the controller.**

I. Introduction

COMMERCIAL transport airplanes use electrical and pneumatic power supplied by engine driven components during inflight operations. However, ground operations and backup power requirements impose the need for an alternate power source called an auxiliary power unit (APU). The APU is a gas turbine engine, usually mounted in the rear of the airplane, which contains an electrical generator and pneumatic source. While the airplane is on the ground, the APU is frequently utilized to supply electrical and pneumatic power (air conditioning) during passenger and cargo loading. Inflight, the electrical and pneumatic power capability of the APU can be used as a backup to main engine driven generators and engine bleed air.

Traditionally, the APU has been started via a series-wound dc motor using power from either an aircraft battery, or a transformer-rectifier unit. However, the dc motor is a high maintenance item for airlines. Frequent removals result due to brush and commutator wear associated with a dc motor. Also, clutches and gears necessary to couple the mechanical power of the dc motor to the APU are failure prone equipment.

An alternate starting method has been developed where the APU generator, already a component of the APU, is used as a synchronous motor to start the APU. This requires the addition of a synchronous motor drive to provide variable frequency power to the synchronous motor. However, it results in the elimination of the dc motor and associated brushes, clutch, and gearing.

This paper discusses an algorithm used by the motor drive that provides control of the starter/generator without relying on measurement of rotor position or machine flux. Until recently, control of such synchronous motor drives utilized a dc current link. Triggering of the converter switches (thyristors) was accomplished maintaining a specified relationship with respect to the motor internal EMF which, in turn, was traditionally determined by means of a rotor angular position sensor [1], [2]. Alternatively, it was shown that using the terminal voltages of the machine as the synchronizing signals is possible instead, thus eliminating need for the shaft position detector [3]–[5] However, these works as well as other papers on control of synchronous motor drives, are concerned with traditional dc current link systems rather than modern dc voltage link systems with PWM control of the motor phase currents.

In this paper, a control suitable for implementation on such equipment using sensorless techniques together with field oriented control is presented. A sensorless approach, in particular, has a number of advantages for this application, the prime of which is the weight saving of the position sensor and its associated wirings. Furthermore, the APU resides in a location associated with relatively harsh environmental and mechanical conditions including temperature extremes, high vibration, and oil. Additional sensors would likely reduce the overall system reliability. In addition, it would be desirable to implement this starting scheme with existing APU's in the field. Requiring a generator for the APU different from the original generator, that is often the same as those on the main engines, may introduce a logistics problem for airlines. Also, additional wiring associated with rotor position or speed sensors would have to be installed in the airplane. Additional wiring is undesirable for an existing airplane due to its installation costs.

Further aspects of airplane APU starting using a converter and the existing generator are discussed in [6].

II. Control System Description

Fig. 1 shows the structure of the proposed control system for the synchronous machine drive. Power to the starter/generator is provided by a three-phase, variable voltage, and frequency pulse-width-modulated (PWM) static inverter. It is expected that the scheme described would be amenable to other forms of static inverters, e.g., six or twelve step inverters. However, the PWM inverter is preferable since it eliminates the higher

Paper IPCSD 95–04, approved by the Industrial Drives Committee of the IEEE Industry Applications Society for presentation at the 1994 IEEE Industry Applications Society Annual Meeting, Denver, CO, October 2–7. Manuscript released for publication January 6, 1995.

F. Nozari and P. A. Mezs are with the Boeing Commercial Airplane Company, Seattle, WA 98124-2207 USA.

A. L. Julian, C. Sun, and T. A. Lipo are with the Department of Electrical and Computer Engineering, University of Wisconsin, Madison, WI 53706 USA.

IEEE Log Number 9411113.

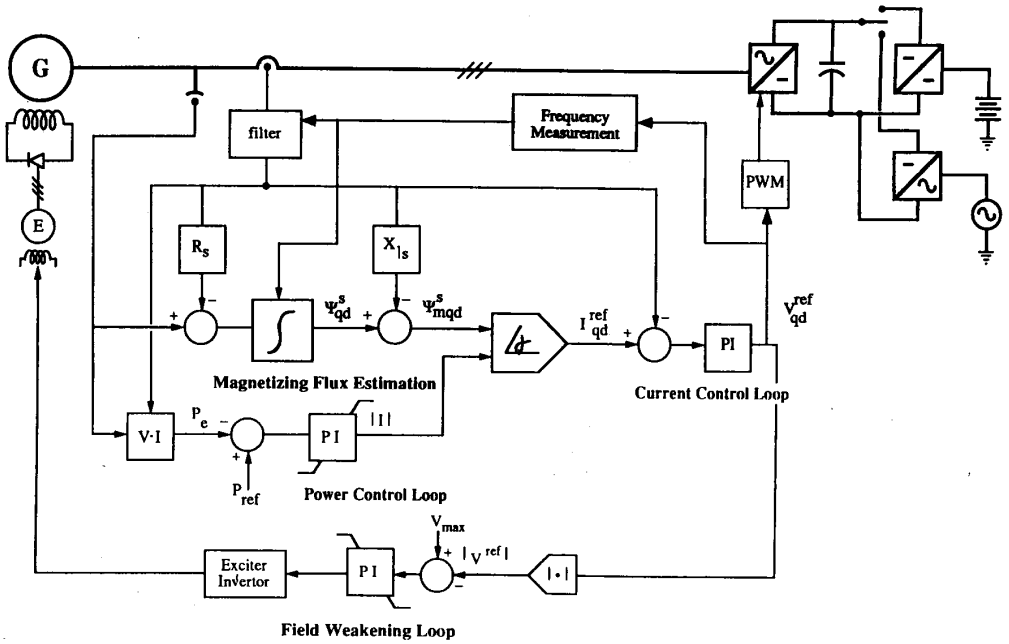

Fig. 1. Synchronous motor drive system.

torque pulsations inherent in other types of inverters. Machine excitation is provided by a separate supply.

In order to maximize the torque per field and armature ampere of the synchronous machine, it is necessary to control the spatial relationship between flux and current phasors in the machine. The phasors of primary importance are the airgap magnetizing flux, Ψ^s_{qdm}, and the stator current, I^s_{qd}, both represented in the stationary reference frame. By maintaining a desired phase angle between these phasors, the developed torque can be controlled and optimized. For a round-rotor synchronous machine, the optimum spatial relationship is to have the stator current in the rotor reference frame, I^r_{qd}, entirely in the q-axis. However, for a salient pole synchronous machine, the optimum spatial separation depends on whether the machine is saturated or not. For the unsaturated condition, the optimum angle, δ, is somewhat less than 90 electrical degrees, and is given by

$$\delta = \alpha - \tan^{-1} \frac{X_{mq} I^r_{qs}}{X_{md}(I^r_{qs} + I_f)} \tag{1a}$$

where the angle α is determined by solving (2a) (derived in the Appendix) and is the angle between I^s_{qd} and the d-axis as shown in Fig. 2. Nomenclature used in the equation, as well as in the remainder of the paper, are an adaptation of that used by Krause [7].

$$(X_{md} - X_{mq}) {I^s_{qd}}^2 \cos 2\alpha + X_{md} I^s_{qd} I_f \cos \alpha = 0. \tag{2a}$$

For a saturated salient pole synchronous machine, on the other hand, the optimum angle is somewhat greater than 90°, and is given by

$$\delta = \alpha - \tan^{-1} \frac{X_{mq} I^r_{qs}}{E_i} \tag{1b}$$

where E_i is the machine internal voltage and the angle α is determined by solving (2b) (derived in the Appendix).

$$E_i \cos \alpha - X_{mq} {I^s_{qd}}^2 \cos 2\alpha = 0. \tag{2b}$$

The control system attempts to maintain a practical approximation to the optimal spatial relationship via control of the static inverter's output current into the synchronous machine terminals.

The magnitude of the desired current vector is determined by the "Power Control Loop" of Fig. 1 that calculates the

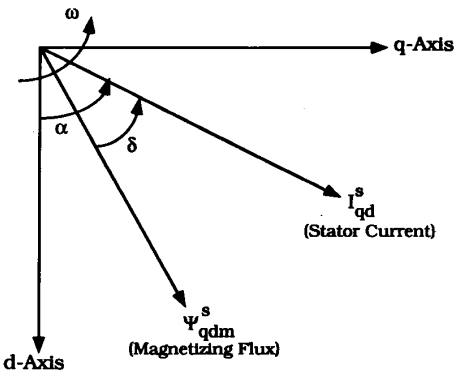

Fig. 2. Relationship between space vectors.

required current magnitude by regulating the input power of the machine to a reference level. The calculated current magnitude is then used to determine a current reference signal, I_{qd}^{ref} in a near optimal spatial relationship to the estimated magnetizing flux, Ψ_{qdm}^{s} that is calculated in the "Flux Estimation" block of Fig. 1.

The "Current Control Loop" regulates the machine current to the above reference current by developing a reference voltage, V_{qd}^{ref}, for the PWM inverter which, in turn, energizes the generator by a PWM voltage proportional to V_{qd}^{ref}.

As the speed of the synchronous machine increases during the start period, the machine's increasing back-EMF requires that the inverter's output voltage be increased in order to regulate the starter/generator current to the reference value of I_{qd}^{ref}. At a certain speed the required voltage may exceed the voltage capability of the inverter. This would cause the inverter to lose the ability to control the motor in the desired fashion. To avoid this loss of control, the excitation to the synchronous machine is reduced after a certain value of line voltage is sensed. This decrease in excitation reduces the back-EMF allowing the inverter to retain control of the starter/generator current at high speeds. The decrease in excitation is accomplished by the "Field Weakening Loop" of Fig. 1.

More detailed information on the individual blocks of the control system are described below.

A. Magnetizing Flux Estimation

One of the most important functions of the proposed control system is to determine the magnitude and angle of the air gap flux vector Ψ_{qdm}^{s}. This function is accomplished within the "Magnetizing Flux Estimation" block.

Determination of Ψ_{qdm}^{s} is accomplished by manipulation of the following well-known synchronous machine equations [3] in a stationary reference frame:

$$V_{qs}^{s} = R_s I_{qs}^{s} + \frac{1}{\omega_b} p\Psi_{qs}^{s} \tag{3}$$

$$V_{ds}^{s} = R_s I_{ds}^{s} + \frac{1}{\omega_b} p\Psi_{ds}^{s} \tag{4}$$

$$\Psi_{mq}^{s} = \Psi_{qs}^{s} - X_{ls} I_{qs}^{s} \tag{5}$$

$$\Psi_{md}^{s} = \Psi_{ds}^{s} - X_{ls} I_{ds}^{s} \tag{6}$$

$$\Psi_{qdm}^{s} = \sqrt{{\Psi_{mq}^{s}}^2 + {\Psi_{md}^{s}}^2} \quad \angle\left(\tan^{-1}\frac{\Psi_{md}^{s}}{\Psi_{mq}^{s}}\right). \tag{7}$$

Determination of the magnetizing flux in the fashion described is marginally stable and would often become unstable due to other system dynamics. A method to stabilize flux estimation is described in Section II-D. In addition, the above equations require knowing the fundamental frequency current components I_{qs}^{s} and I_{ds}^{s}. Finding these current components for a relatively large sized generator is complicated by the fact that the actual current waveforms have significant high order harmonic content. Simulation studies indicate that the relatively small impedance of large generators may not provide inherent filtering of the harmonic content. Hence, direct use of the actual current waveforms without filtering the harmonics would result in degradation of system operation. The control system would then try to respond to the harmonic components in addition to the fundamental. Extraction of this fundamental component is accomplished by a current measurement filter.

B. Current Measurement Filter

As discussed above, simulation studies indicate that filtering of the machine input current may be an important element. Inadequate filtering may result in unacceptable flux estimation, current control, and PWM converter operation. This is somewhat contrary to what has been observed in typical drive system applications using induction machines in which the armature winding series inductance provides sufficient filtering of harmonic currents. As noted earlier, synchronous machines of high rating may not have as high a series impedance to provide inherent filtering action. Consequently, a filter may be necessary for acceptable operation. The filter must effectively attenuate high order harmonic currents without introducing significant phase lag in the measured armature fundamental frequency current. In order to eliminate the harmonic components from the control system, a narrowband filter tuned to the system fundamental frequency is used. The mathematical representation of this filter is given by

$$\frac{I_{\text{fund}}}{I_{\text{actual}}} = \frac{2\zeta\omega_r s}{\omega_r^2 + 2\zeta\omega_r s + s^2} \tag{8}$$

where ω_r is the machine's electrical angular speed, proportional to the system fundamental frequency. This filter has a unity gain and zero phase shift at its central frequency, i.e., the system fundamental frequency, and a sharply reduced gain at all other frequencies, hence it would provide the desired filtering. Also note that since the frequency of the fundamental component changes with machine speed, the filter's central frequency must change with machine speed. The filter's central frequency is determined by measuring the fundamental frequency of the supplied PWM voltage as described in the following section.

C. Determination of Electrical Frequency of the Machine

As the above description indicates, determination of the machine's electrical angular speed, ω_r, is critical for operation of the control system. In the proposed scheme this is accomplished without sensing the machine's shaft speed. Instead it is determined mathematically using a well-known phase-locked loop approach [8]. The block diagram is shown in Fig. 3.

Voltage signals V_{ds}^{s} and V_{qs}^{s} which are proportional to $\cos\theta_e$ and $\sin\theta_e$, are inputs to the phase locked circuit. These voltages are derived from the PWM reference voltages and are combined with $\cos\theta$ and $\sin\theta$ terms generated by the local phase-locked oscillator. This multiplication and subsequent subtraction results in a signal proportional to $\sin(\theta_e - \theta)$. If $\theta_e - \theta$ is very small, the $\sin(\theta_e - \theta)$ term represents a very slowly varying sine wave. Feeding this input to a PI controller results in a change in the controller's output, ω, until $\theta_e - \theta$ becomes zero. At this point the $\sin(\theta_e - \theta)$ term equals zero, and the integrator's output remains locked onto $\omega_e (= d\theta_e/dt)$. This method depends on the value of ω being reasonably close to ω_e so that the argument of the sine term is small. Otherwise, the $\sin(\theta_e - \theta)$ term becomes oscillatory and the error term

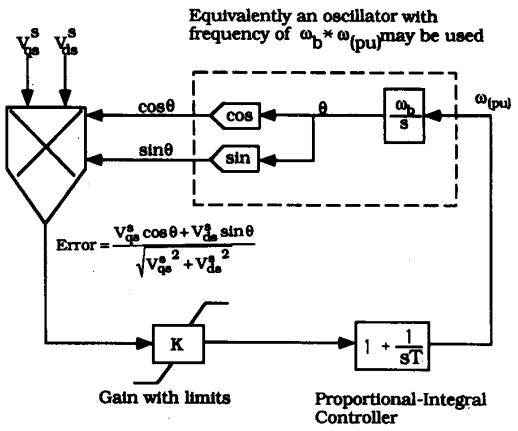

Fig. 3. Phase-locked loop technique to measure rotor speed.

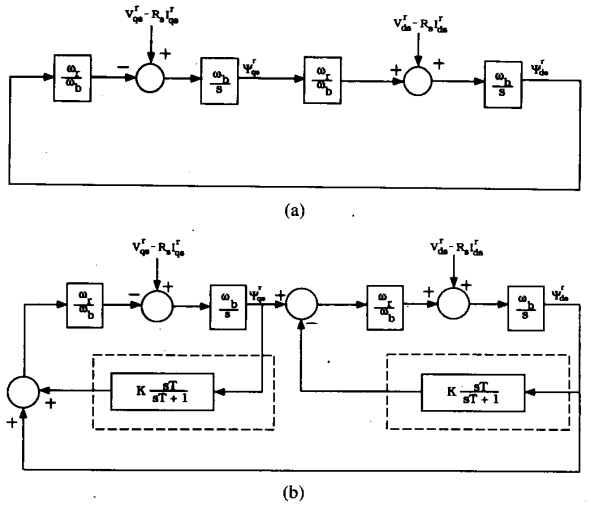

Fig. 4. Stabilization of synchronous machine equations. (a) Block diagram of original equations showing them to be equivalent to an oscillator. (b) Block diagram of synchronous machine flux estimation equations with addition of stabilization loops (in dotted lines).

may not be decreased by the rest of the loop to zero. In the machine start system described herein we know that initially $\omega_e = 0$. This information is used to initialize the electrical angular velocity continually as the machine speeds up. Other forms of phase-locked loop "acquisition" techniques need to be investigated for a more robust frequency measurement.

D. Stabilization of the Flux Estimation Loop

As mentioned in Section II-A, the flux estimation loop is marginally stable and would often become unstable due to other system dynamics. In order to see this marginal stability, it is instructive to transform the flux equations (3) and (4) to the rotor reference frame and arrange them as

$$\frac{1}{\omega_b} p\Psi_{qs}^r = V_{qs}^r - R_s I_{qs}^r - \left(\frac{\omega_r}{\omega_b}\right)\Psi_{ds}^r \tag{9}$$

$$\frac{1}{\omega_b} p\Psi_{ds}^r = V_{ds}^r - R_s I_{ds}^r + \left(\frac{\omega_r}{\omega_b}\right)\Psi_{qs}^r. \tag{10}$$

The fact that the poles of these equations lie near the imaginary axis means that the system is marginally stable. Other system dynamics may push these poles into the right-half plane thus making the overall system unstable. It would be desirable to move these poles into the left half plane to stabilize these equations without impacting the steady-state and low frequency values of the flux estimates.

To solve this instability problem, feedback loops of washout form have been included in the flux estimation portion. These feedback loops are shown in Fig. 4 and result in movement of the poles to the left half plane. This shift in the poles causes damping of high-frequency transient components, but it does not impact the steady-state and low-frequency response of the flux estimator. The steady-state value of the flux estimator will continue to show the correct value. The flux estimator equations in the rotor reference frame are

$$\frac{1}{\omega_b} p\hat{\Psi}_{qs}^r = V_{qs}^r - R_s I_{qs}^r - \frac{\omega_r}{\omega_b}[\hat{\Psi}_{ds}^r + K(\hat{\Psi}_{qs}^r - \sigma_{qs}^r)] \tag{11a}$$

$$\frac{1}{\omega_b} p\hat{\Psi}_{ds}^r = V_{ds}^r - R_s I_{ds}^r + \frac{\omega_r}{\omega_b}[\hat{\Psi}_{qs}^r - K(\hat{\Psi}_{ds}^r - \sigma_{ds}^r)] \tag{12a}$$

$$p\sigma_{qs}^r = \frac{1}{T}(\hat{\Psi}_{qs}^r - \sigma_{qs}^r) \tag{13a}$$

$$p\sigma_{ds}^r = \frac{1}{T}(\hat{\Psi}_{ds}^r - \sigma_{ds}^r) \tag{14a}$$

where K, T, σ_{qs}^r, and σ_{ds}^r are the washout gain, time constant, q- and d-axis state variables, respectively, and the caret (^) denotes an estimated variable. Note that the washout feedback loops are in their simplest form when they are modeled in the rotor reference frame as shown in Fig. 4. For practical reasons they may need to be implemented in the stationary reference frame to eliminate the need for rotor position information. The flux estimator equations in the stationary reference frame are then as follows:

$$\frac{1}{\omega_b} p\hat{\Psi}_{qs}^s = V_{qs}^s - R_s I_{qs}^s - K\frac{\omega_r}{\omega_b}(\hat{\Psi}_{qs}^s - \sigma_{qs}^s) \tag{11b}$$

$$\frac{1}{\omega_b} p\hat{\Psi}_{ds}^s = V_{ds}^s - R_s I_{ds}^s + K\frac{\omega_r}{\omega_b}(\hat{\Psi}_{ds}^s - \sigma_{ds}^s) \tag{12b}$$

$$p\sigma_{qs}^s = \frac{1}{T}(\hat{\Psi}_{qs}^s - \sigma_{qs}^s) + \omega_r \sigma_{ds}^s \tag{13b}$$

$$p\sigma_{ds}^s = \frac{1}{T}(\hat{\Psi}_{ds}^s - \sigma_{ds}^s) - \omega_r \sigma_{qs}^s. \tag{14b}$$

E. Current Control Loop Function

Once the phase angle of $\hat{\Psi}_{qdm}^s$ is known, the desired phase angle of the machine reference current, I_{qd}^{ref}, can be determined. For optimum torque production, the I_{qd}^{ref} should be advanced from $\hat{\Psi}_{qdm}^s$ by the angle δ, which is determined by (1a) or (1b) depending on the machine saturation condition. This requires knowledge of the synchronous machine parameters, in particular, the field circuit resistance to determine the field current I_f and the machine saturation condition. However, this mathematically elegant approach is impractical since the field circuit resistance could significantly change with temperature variations and the resulting field current and

the machine saturation condition could dramatically change. Fortunately, the angle δ is reasonably close to 90 electrical degrees for realistic conditions and does not need to be determined precisely for near optimum operation. In practice, selecting a fixed value of δ between 70 and 110° would result in an acceptable, near optimum performance. Note that for an unsaturated machine, a δ of 90 electrical degrees would not reinforce the magnetizing flux, while a δ less than 90 electrical degrees would reinforce the magnetizing flux and possibly cause saturation. These factors should be considered in selecting a fixed value of δ.

Regulation of I_{qd}^{s} within the "Current Control Loop" is done with currents expressed in the synchronously rotating reference frame. This implementation results in the regulation of dc reference quantities thus overcoming the limitations PI regulators have with ac references [9].

F. Power Control Loop Function

As described before, the magnitude of the reference current, I_{qd}^{ref}, for current control is obtained via the power control loop. Instantaneous machine voltage and the fundamental component of machine current (obtained from the current filter described earlier) are multiplied to obtain instantaneous machine input power, P_e. This power is compared to a given reference power, P_{ref}, and the resulting error is processed by an appropriate controller involving low-pass filtering and PI regulation to determine the magnitude for the reference current. This magnitude information is combined with the desired current phase angle to determine the reference current, I_{qd}^{ref}, which is then compared with the filtered measured currents to form error signals to drive the PI current regulator blocks to produce a reference value for the inverter output voltage, V_{qd}^{ref}. The V_{qd}^{ref} is then converted to phase values, V_{abc}^{ref}, which in turn are inputted to the PWM inverter for appropriate switching actions through triangularized pulse-width-modulation. The V_{qd}^{ref} is also inputted to the frequency measurement block to determine the fundamental frequency of the supplied voltage which is proportional to the machine speed.

G. Field Weakening Loop Function

In order to provide torque control of the synchronous machine at high speeds, it is necessary that the inverter be able to control the required current into the machine windings. As the machine speed increases, the internal voltage of the synchronous machine, caused by field excitation, also increases. In order to counteract this back-EMF, the voltage supplied by the inverter must increase as the machine speed increases. With a constant field excitation, a speed would eventually be reached at which the inverter would be unable to satisfy the commanded current loop unless some means were in place to reduce the synchronous machine internal voltage.

This means is provided by the field weakening loop. Initially the field current is maintained at a maximum possible value to give a strong rotor field and thus a high starting torque. The voltage commanded by the current control loop is sensed during the machine start-up process. When the magnitude of this commanded voltage, V_{qd}^{ref}, exceeds a given reference value, $V_{\max}$, the exciter current is reduced by the field weakening loop. This maintains the machine back-EMF constant as the machine speed increases during the start cycle. This excitation control will extend the speed range that the converter maintains control of the machine during starting.

III. System Start-Up

Unfortunately, since the flux estimator is itself a dynamic system, it takes some time (about six seconds for the example in Section IV) to overcome initial transients and correctly estimate the machine fluxes. Therefore, early in the synchronous machine start-up, another control means should be used to provide starting of the synchronous machine while the flux estimator is reaching the correct estimating condition. Afterward, the flux estimator can be engaged in the preferred start-up mode to provide a near optimum start-up characteristic as described previously.

The following early start-up technique was found effective through computer simulation studies and laboratory tests. The technique is comprised of the following four steps:

1) Energize the synchronous machine's field circuit with a maximum possible field voltage while the stator winding is energized by a very low-frequency voltage (about two hertz for the example) at a very small voltage magnitude determined by a current controller regulating the stator current to its maximum allowable level. The synchronous machine should start rotating at a speed corresponding to the supplied frequency as the machine's field flux increases.
2) After a couple of seconds, when the synchronous machine's field flux is nearly established, ramp-up the inverter output frequency at a fairly slow rate of a few hertz per second (4 Hz/s for the example) to a suitable value (about 20 Hz for the example). The synchronous machine should follow this frequency ramp-up and continue rotating accordingly, in an open loop manner.
3) Allow a few seconds for such an open loop operation mode to provide enough time for the flux estimator to overcome start-up transients and correctly estimate the machine fluxes.
4) Switch to the preferred start-up mode using the flux estimator for near optimum start-up performance.

IV. Simulation Results

A computer simulation of the system as described above was performed for starting an auxiliary power unit with a 90-kVA generator typically installed in mid to large size commercial transport jetliners. The results are shown in Figs. 5 through 24.

Figs. 5 through 9 display voltage and current parameters during the start-up of the synchronous machine. Note the discontinuities at about six seconds due to switching from the early open loop start-up method to the preferred closed loop method. Figs. 5 and 6 show the time history of the reference PWM voltage magnitude and the average PWM inverter output voltage magnitude. It can be seen that the magnitude of the required PWM voltage is small at the beginning of the APU

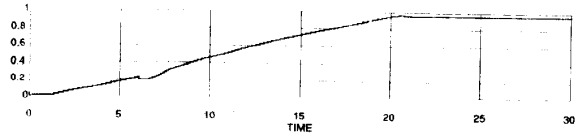

Fig. 5. Reference PWM voltage magnitude (p.u.)

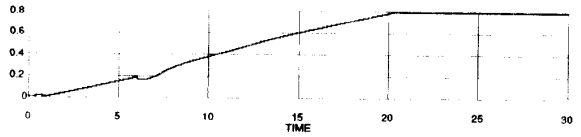

Fig. 6. Average PWM voltage magnitude (p.u.)

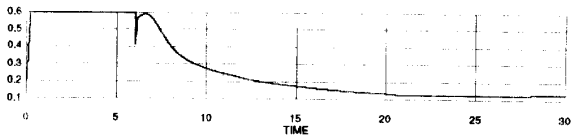

Fig. 7. Reference current magnitude (p.u.)

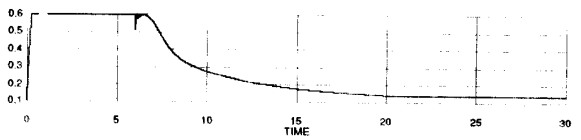

Fig. 8. Actual average current magnitude (p.u.)

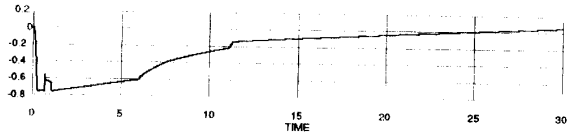

Fig. 9. Drag torque (p.u.) (positive for generator).

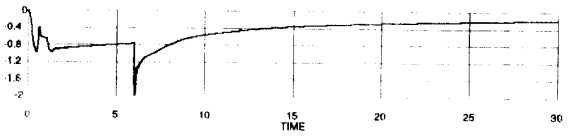

Fig. 10. Average electrical torque (p.u.) (positive for generator).

start-up and rises gradually as the APU speeds up. While the voltage magnitude is less than the PWM maximum limit (this is the reference value of the field weakening loop) the field weakening PI regulator is driven to its upper limit, hence the machine excitation is at its maximum allowable level (see Fig. 21).

Also note that as the machine speed increases, the machine's back-EMF voltage increases. This requires that the PWM inverter reference and output voltages increase to maintain

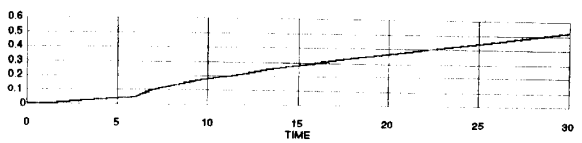

Fig. 11. Rotor speed (p.u.)

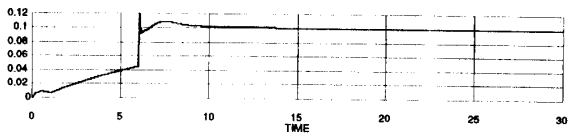

Fig. 12. Average electrical power (p.u.) (positive for motor).

proper current regulation (see Fig. 5). As the PWM reference voltage approaches the PWM maximum limit, the field weakening loop reduces the generator excitation level. The inverter can then maintain control of the machine start as the speed continues to increase.

Figs. 7 and 8 show the time history of the inverter's reference and average current magnitudes. It is noted that early in the start-up the machine power is small due to its low speed, hence, the power controller PI regulator is driven to its upper limit resulting in the maximum allowable machine current. As the machine speeds up, the input power to the machine gradually rises. Upon switching from the early start-up method to the preferred start-up method, the machine input power suddenly increases to the desired value of 0.1 per unit due to the increased machine torque (see Fig. 12). Thereafter, the PI regulator maintains the desired machine input power by reducing the machine current.

Figs. 9 through 12 show the drag torque and the average generator electrical torque during start-up, as well as the generator speed and electrical power. (The torque values in both these figures have a positive reference for generator produced torques and therefore have negative values for the rotor torque that was simulated).

The electrical torque, during the early start-up, overcomes the drag torque, resulting in a modest acceleration. During the preferred start-up method, however, the start-up torque is substantially higher, thereby, resulting in an increased acceleration. As the power controller loop starts to reduce the generator armature current, the electrical torque is also reduced.

Figs. 13 through 16 show the reference and the actual PWM voltages, as well as the actual and filtered synchronous machine armature currents at about 20 s into the machine's start-up, respectively.

Fig. 13 is the reference input voltage to the PWM inverter, while Fig. 14 is the resulting inverter voltage. Figs. 15 and 16 are the input and output of the narrow-band filter, respectively. As these figures indicate, the filter performance is excellent. The filter eliminates undesirable harmonics without introducing any phase lag into the fundamental component. Note that in the simulation study neither an electromagnetic interference (EMI) filter nor the APU generator feeders were considered.

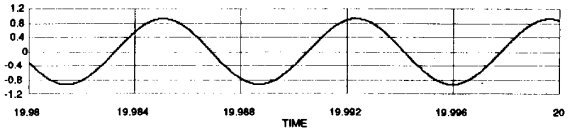

Fig. 13. Reference PWM voltage (p.u.)

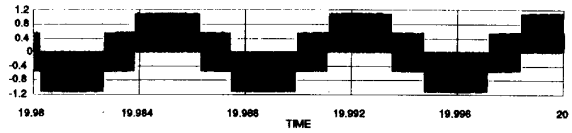

Fig. 14. Actual PWM voltage (p.u.)

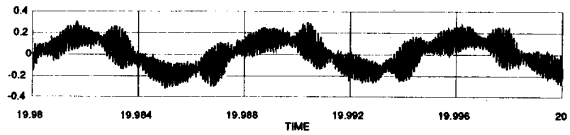

Fig. 15. Actual current (p.u.)

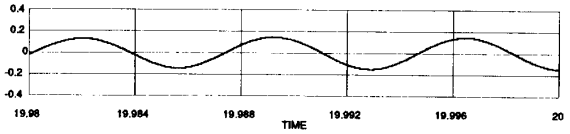

Fig. 16. Filtered current (p.u.)

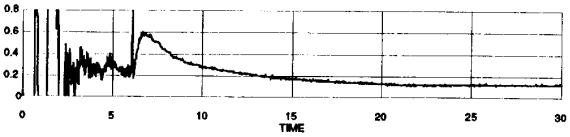

Fig. 17. Estimated q-axis magnetizing flux (p.u.)

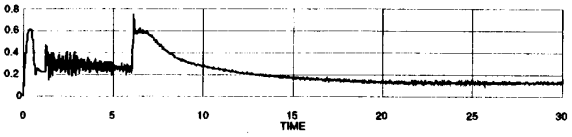

Fig. 18. Actual q-axis magnetizing flux (p.u.)

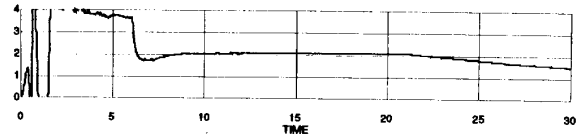

Fig. 19. Estimated d-axis magnetizing flux (p.u.)

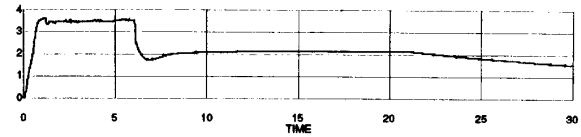

Fig. 20. Actual d-axis magnetizing flux (p.u.)

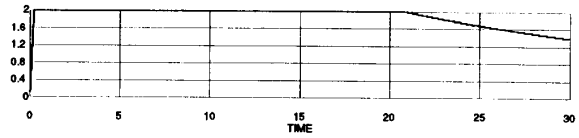

Fig. 21. Field voltage (p.u.)

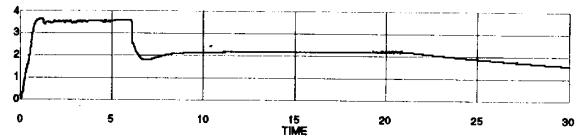

Fig. 22. Field flux (p.u.)

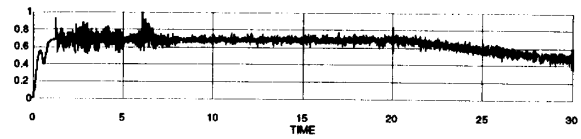

Fig. 23. Field current (p.u.)

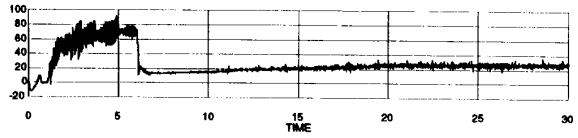

Fig. 24. Power factor angle (degree).

It is expected that both these may significantly impact the characteristics of these undesirable harmonics.

Figs. 17 through 20 display the time history of the actual and estimated values of q- and d-axis magnetizing flux during the start-up. The estimated values are obtained from the "Magnetizing Flux Estimation" block.

After attenuation of start-up transients in the flux estimator, which takes about five seconds, the estimated and actual magnetizing flux values are in close agreement. They continue to track each other throughout the rest of the machine start period.

Figs. 21 through 24 show the time history of the field voltage, flux, and current in per-unit. The power factor input to the machine is also shown. The "Field Weakening Loop" is seen to take effect approximately 21 s into the machine start. At this time the field voltage, flux, and current start to decrease as the machine speed increases.

The computer simulations verified proper operation of the generator/start motor drive system and its ability to quickly

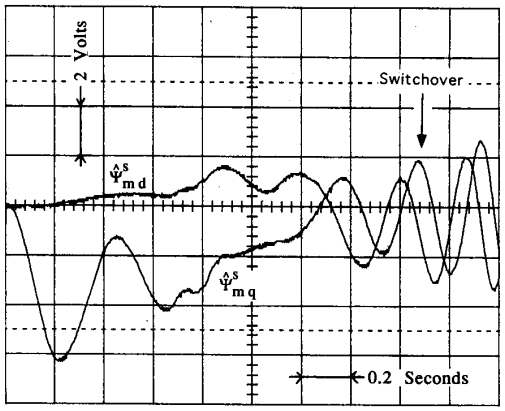

Fig. 25. Air gap flux estimated variables Ψ^s_{md} and Ψ^s_{mq} before and immediately after switchover to closed loop control.

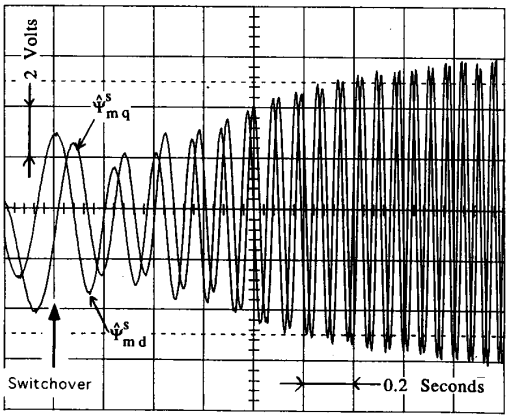

Fig. 27. Air gap flux estimated variables Ψ^s_{md} and Ψ^s_{mq} just before and after switchover to closed loop control.

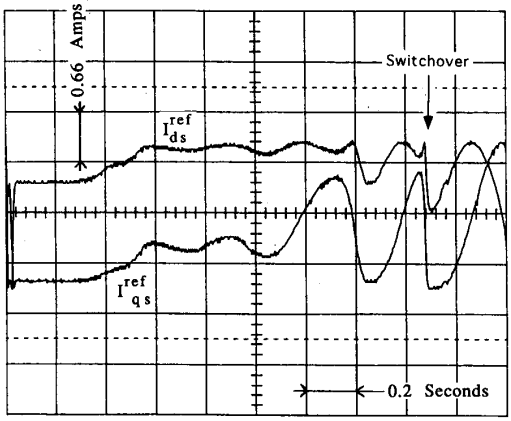

Fig. 26. Reference d- and q-axis currents I^{ref}_{ds} and I^{ref}_{qs} corresponding to Fig. 25 obtained from the open loop calculation before switchover and from the flux estimator after switchover.

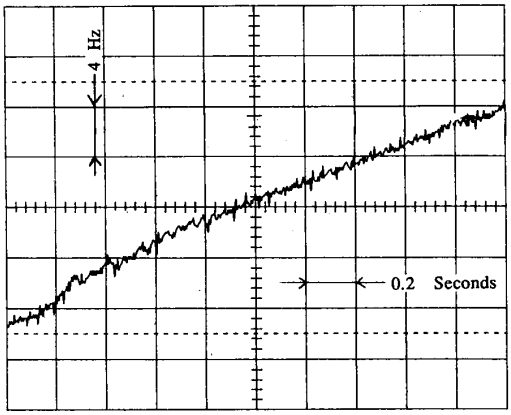

Fig. 28. Variation in rotor speed for the case where $\delta = 25°$.

bring the APU to rated speed. Time to starter cutout using the system proposed in this paper was approximately 30 s. In the present system which uses a dc start motor, the time to starter cutout, under identical conditions, can take up to 2 min. This shows the increased capability of the proposed starting system.

V. Hardware Implementation of Proposed Synchronous Machine Starting System

A synchronous machine with drive converter, using the scheme described herein, was constructed at the University of Wisconsin-Madison. Operation of this system verified successful starting of the synchronous machine without rotor position sensing, and was insensitive to parameter variation.

The system used to implement this starting scheme was a three-phase, four-pole, salient pole, synchronous motor rated at 3 hp. The machine was controlled using a digital signal processor which, in turn, controlled the output currents of a three-phase voltage source inverter.

During the tests the field voltage was maintained at a constant level during all acceleration cycles. The fundamental frequency was increased from 0 to 4 Hz in approximately 1.8 s. Once the 4 Hz operating point was reached, the flux estimator was used to define the reference currents. This two step process allowed the transients in the flux estimator to decay before using these signals actively in the closed loop control. Fig. 25 shows a typical trace of the d- and q-axis flux estimators from the point of energization until 2 s. A transition from open loop to closed loop flux control is implemented at 1.67 s, marked appropriately on Fig. 25 with an arrow. Fig. 26 shows the resulting commanded currents corresponding to Fig. 25. Fig. 27 covers a later portion of acceleration interval where the transition is made at the same instant at for Fig. 25 but appearing as 0.2 s on this trace (again marked by an arrow). The trace shows the remainder of a typical acceleration period demonstrating very satisfactory estimation of the magnetizing flux when the loop is closed. Again at the switchover point, the current is quickly regulated to the proper value.

As part of the study, the torque angle was varied to observe the changes of the acceleration. The speed profiles

demonstrated that the developed torque can be controlled over a wide range by controlling the phase angle between the flux and current as predicted. For example, Fig. 28 shows the speed for the case where the torque angle δ is held constant at 25° with constant armature current. It can be observed that the speed changes linearly which indicates that the torque is being held constant while the rotor accelerates. Other values for constant δ show similar linear behavior of speed with constant current. The results demonstrate that further refinement of the software for a specific machine should readily lead to the correct algorithm for a maximum torque per armature current.

The hardware implementation has demonstrated the feasibility of the control algorithm. In particular, the wash-out based stabilizing feedback loops to the flux estimator have been shown to realize a stable field control algorithm. The entire system was implemented without the need for a rotor position sensor. This approach has been demonstrated to enable the torque angle to be accurately controlled during the acceleration of a synchronous machine. A change of stator resistance and leakage inductance estimates used in the flux estimator over a four to one range showed virtually no change to the starting characteristics of the machine. It should be mentioned that numerous acceleration cycles were tested. None of these tests indicated marginally stable or unstable behavior.

VI. Conclusion

A method of starting an airplane's APU through the synchronous generator mounted on the unit has been presented. The method does not require sensing of the machine's rotor speed or position. Deletion of these sensors should add to the reliability of the system due to the relatively harsh operating environment of the APU. Computer simulations and laboratory test results have verified that the proposed scheme is stable, robust, and virtually insensitive to variation of synchronous machine parameters.

Appendix
Derivation of Equation Giving Maximum Torque Angle for a Salient-Pole Machine

The basic torque equation in per unit is

$$T_{pu} = \Psi^r_{md} I^r_{qs} - \Psi^r_{mq} I^r_{ds} \tag{A1}$$

where Ψ^r_{mq} and Ψ^r_{md} are rotor reference q- and d-axis components of magnetizing flux respectively, while, I^r_{qs} and I^r_{ds} are rotor reference q- and d-axis components of stator current, respectively.

For an unsaturated machine, the above equation can be expanded as

$$T_{pu} = X_{md}(I^r_{ds} + I_f) I^r_{qs} - X_{mq} I^r_{qs} I^r_{ds} \tag{A2}$$

where I_f, X_{mq}, and X_{md} are the machine's field current, q-axis and d-axis magnetizing reactances, respectively.

By referring to Fig. 2, the above equation can be expanded as

$$T_{pu} = (X_{md} - X_{mq}) {I^s_{qd}}^2 \sin\alpha\cos\alpha + X_{md} I_f I^s_{qd} \sin\alpha. \tag{A3}$$

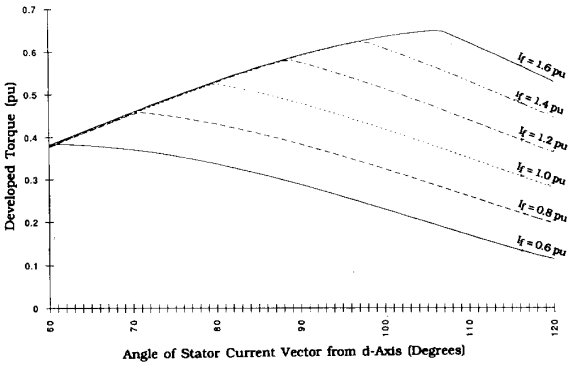

Fig. 29. Torque angle characteristics of a typical synchronous machine for 0.5-p.u. stator current.

The maximum torque occurs at angle α which can be determined by calculating $dT_{pu}/d\alpha$ and equating it to zero. The resulting transcendental equation is (2a).

For a salient pole saturated synchronous machine, it can be assumed that the saturation only occurs in the d-axis. The basic torque equation (A1) can then be expanded as

$$T_{pu} = E_i I_{qs} - X_{mq} I^r_{qs} I^r_{ds} \tag{A4}$$

where E_i is the saturated generator internal voltage which may be assumed constant due to the d-axis saturation. By referring to Fig. 2, this equation can be expanded as

$$T_{pu} = E_i I^s_{qd} \sin\alpha - X_{mq} {I^s_{qd}}^2 \sin\alpha\cos\alpha. \tag{A5}$$

The maximum torque occurs at angle α which can be determined by taking the derivative of (A5) with respect to α and equating it to zero. The result is (2b).

Fig. 29 displays torque versus δ for several values of I_f. Larger values of I_f would tend to drive the synchronous machine into saturation which would result in the optimum δ being larger than 90°.

References

[1] A. Habock and D. Kollensperger, "Application and further development of converter-fed synchronous motors with self-control," *Siemens Rev.*, vol. 38, no. 9, pp. 393–395, 1971.
[2] N. Sato and V. V. Semenov, "Adjustable speed drive with a brushless dc motor," *IEEE Trans. Ind. General Applicat.*, vol. IGA-7, pp. 539–543, 1972.
[3] A. B. Plunkett and F. G. Turnbull, "Load commutated inverter/synchronous motor drive without a shaft position sensor," *IEEE Trans. Ind. Applicat.*, vol. IA-15, no. 1, pp. 63–71, Jan./Feb. 1979.
[4] H. Le-Huy, A. Jakubowicz, and R. Perret, "A self-controlled synchronous motor drive using terminal voltage system," *IEEE Trans. Ind. Applicat.*, vol. IA-18, no. 1, pp. 46–53, Jan./Feb. 1982.
[5] J. Davoine, R. Perret, and H. Le-Huy, "Operation of a self-controlled synchronous motor without a shaft position sensor," *IEEE Trans. Ind. Applicat.*, vol. IA-19, no. 2, pp. 217–222, Mar./Apr. 1983.
[6] T. S. Latos and M. J. McArthur, "System design considerations for an APU starter-generator," presented at the 1993 SAE Aerotech Conf.
[7] P. C. Krause, *Analysis of Electric Machinery*. New York: McGraw-Hill, 1986.
[8] D. H. Wolaver, *Phase-Locked Loop Circuit Design*. Englewood Cliffs, NJ: Prentice-Hall, 1991.
[9] T. M. Rowan and R. J. Kerkman, "A new synchronous current regulator and an analysis of current-regulated PWM inverters," *IEEE Trans. Ind. Applicat.*, vol. IA-22, no. 4, pp. 678–690, July/Aug. 1986.

Farhad Nozari (S'74–M'76–SM'84) received the B.S. degree from the University of Teheran, Iran, the M.S. degree from the University of Southern California, Los Angeles, and the Ph.D. degree from Purdue University, West Lafayette, IN, all in electrical engineering.

He had been on the faculty of the University of Michigan, Ann Arbor, and Purdue University. He was a Research Assistant at the University of Southern California and Purdue University, and a Design Engineer at several consulting engineering firms in California and Iran. In 1978, he joined General Electric Company, Schenectady, NY, where he was a Senior Application Engineer in the Power Systems Engineering Department. He was involved in many projects concerning high voltage dc and static var systems and their impacts on the stability of associated power systems. He has developed load modeling techniques for transient stability studeies and control strategies for multiterminal dc systems and HVDC applications in weak ac systems. He has also conducted power system studies for several HVDC and static var compensation applications. In 1989, he joined the Boeing Company, Seattle, WA, where he worked in Boeing Computer Services, in which he was involved in control systems analysis and development of advanced mathematical algorithms for the Boeing "Catia man." He is currently a Senior Principal Engineer in the Electric Research and Development component of the Boeing Commerical Airplane Group, where he is involved in the development of advanced electrical power systems for use on future ariplanes. He has developed control techniques for starting the airplane's auxiliary power unit and for operating the airplane hydraulic pumps, as well as techniques for analysis and simulation of aircraft power systems. His areas of interest include modeling and analysis of power system components, development of new mathematical softwares, and modern control theory. He has had more than 25 years of research and system study experience in different aspects of electrical power systems and 5 years of experience in the design of power distributions systems. His work has resulted in methodologies for analysis and design of power system components. He has authored or coauthored about 25 papers in the area of analysis and simulation of power systems.

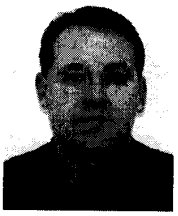

Paul A. Mezs (M'91) received the B.S.E.E. degree from the University of Washington, Seattle, in 1980.

Since 1980, he has been with the Boeing Commercial Airplane Group, where he has been responsible for the design, testing, and certification of aircraft electrical power systems and components for the 737 and 757 airplanes. He was a member of the team which certified a variable-speed-constant-frequency (VSCF) generation system on the 737 airplane in 1989. From 1989 to 1994, he served as a designated engineering representative to the Federal Aviation Administration. Since 1991, he has worked in the electrical Research and Development Group to develop advanced electrical power systems for use on future airplanes. His main areas of interest are power electronics, electrical machines, and drives used for their control.

Alexander L. Julian was born in Palo Alto, CA, in 1962. He received the bachelor's and Master's degrees from the University of Missouri, Columbia, in 1992.

He was a research assistant at the Power Electronics Research Center, headed by Prof. R. G. Hoft. Currently, he is pursuing the Ph.D. degree at the Wisconsin Power Electronics Research Center, University of Wisconsin, Madison, WI.

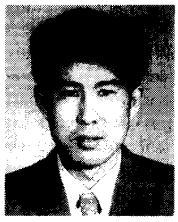

Chiping Sun received the B.S.E.E. and the M.S.E.E. degrees from the Harbin Institute of Electrical Technology, China, in 1982 and 1988, respectively.

He was teaching and doing research at the Department of Electrical Engineering, Harbin Institute of Electrical Technology for eight years. He then joined the Wisconsin Electric Machine and Power Electronics Consortium, University of Wisconsin, Madison, as a research associate. He is interested in the areas of electric machine controls, ac motor drives, power electronics, and industrial processing controls. He has published more than 13 papers.

Mr. Sun received the First Prize Paper from the Industrial Drives Committee at the 1993 IEEE Industry Applications Soceity Annual Meeting.

Thomas A. Lipo (M'64–SM'71–F'87) is a native of Milwaukee, WI. He received the B.E.E. and M.S.E.E. degrees from Marquette University, Milwaukee, in 1962 and 1964, respectively, and the Ph.D. degree in electrical engineering from the University of Wisconsin, Madison, in 1968.

From 1969 to 1979, he was an Electrical Engineer in the Power Electronics Laboratory of Corporate Research and Development, General Electric Company, Schenectady, NY. He became Professor of Electrical Engineering at Purdue University, West Lafayette, IN, in 1979. In 1981, he joined the University of Wisconsin, Madison, as Professor of Electrical Engineering, and where he is presently the W. W. Grainger Professor for Power Electronics and Electrical Machines.

Dr. Lipo received the Outstanding Achievement Award in 1986 from the IEEE Industry Applications Society for his contributions to the field of ac drives. In 1990, he received the William E. Newell Award from the IEEE Power Electronics Society for contributions to the field of power electronics. He has been selected to receive the 1995 Nicola Tesla IEEE Field Award. He has served in various capacities for three IEEE societies, including President of the Industry Applications Society in 1994.